

The Dependence of the Discharge Coefficient on Density Contrast - Experimental Measurements

Joanne M. Holford¹ and Gary R. Hunt²

¹Department of Applied Mathematics & Theoretical Physics, University of Cambridge, Silver Street, Cambridge, CB3 9EW, UK.

²Department of Civil & Environmental Engineering, Imperial College of Science, Technology and Medicine, London, SW7 2BU, UK.

Abstract

The discharge coefficient C_d associated with a strongly contracting flow through a sharp-edged orifice is, in general, assumed to be constant at sufficiently high Reynolds numbers. The effect of buoyancy forces due to a difference in density between the fluids on either side of the opening is typically ignored. In the absence of a buoyancy contrast, the discharging flow contracts due to inertial effects giving $C_d \approx 0.6$. We hypothesise that a density contrast may cause a significant reduction in C_d for flows through horizontally or vertically orientated openings. We test this hypothesis by deducing C_d from laboratory measurement of the volume flow rate driven through an opening by hydrostatic pressure differences in a two-layer saline stratification in water.

Plume theory shows that a discharge of buoyant fluid from an area source may contract in addition to the inertial contraction. The discharge through a horizontal or vertical opening is characterised by conditions at the opening, represented by the dimensionless discharge parameter Γ_d , which is a function of the volume, buoyancy and momentum fluxes at the opening. For horizontal openings, once a critical value of Γ_d is exceeded, C_d exhibits a strong dependence on the density contrast and decreases rapidly with increasing Γ_d . For vertical openings, C_d decreases with Γ_d , for all Γ_d . The dependence of C_d on density contrast implies a potential for serious errors in the prediction of volume flow rates through constrictions if a constant value of C_d is assumed, as is current practice.

Introduction

Internal flows through sudden contractions are encountered in many engineering and environmental flow situations. For example, the flow rate through a pipe may be calculated by inserting an orifice plate to reduce the cross-sectional area, and measuring the pressure drop across the plate (Ward-Smith [11]). A pressure drop also occurs when the air stream through a building contracts to pass through a window or door opening.

For sufficiently high Reynolds numbers Re (≥ 4000 , see Ward-Smith [11]), the pipe flow of a homogeneous fluid through a sharp-edged opening has the same general features regardless of the details of the opening geometry. The flow accelerates as it contracts from the pipe of area A/λ , through the orifice of area A , and continues to contract to a minimum cross-sectional area of A_{vc} at the *vena contracta*, see figure 1a. As the area ratio $\lambda \rightarrow 0$, the area of the pipe becomes much larger than the orifice.

Assuming a uniform velocity profile across the opening and no subsequent contraction, inviscid flow theory (Batchelor [1]) shows that the maximum volume flow rate Q_{max} is given by

$$Q_{max} = A \sqrt{2\Delta p / \rho_0}, \quad (1)$$

where Δp is the driving pressure drop and ρ_0 is the fluid density.

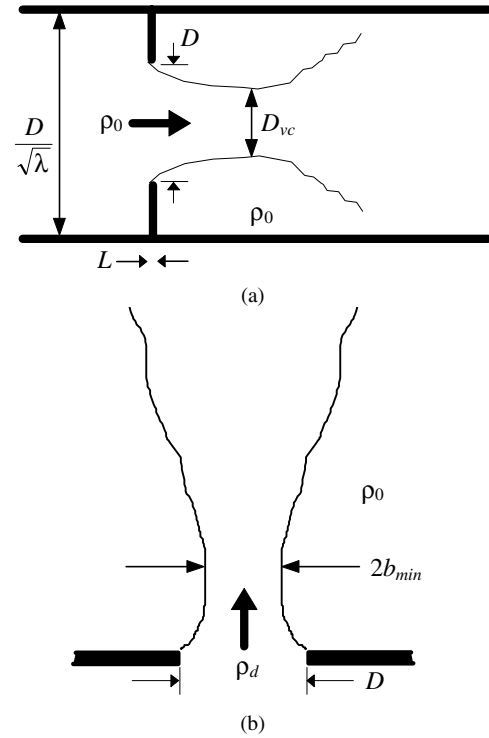


Figure 1. Schematics of the flow through a sudden contraction, direction of flow indicated by the heavy arrows. (a) A high Reynolds number flow of homogeneous fluid through an orifice in a pipe (D_{vc} denotes the hydraulic diameter of the jet at the *vena contracta*). The flow pattern is independent of the orientation of the pipe. (b) A buoyant discharge through a horizontal opening.

The actual flow rate Q may also depend on the fluid viscosity ν , opening surface roughness ϵ , opening thickness L , and the area ratio λ , so that $Q = f(A, \Delta p, \rho_0, \nu, \epsilon, L, \lambda)$, for some function f . On dimensional grounds we expect

$$\frac{Q}{Q_{max}} = C_d \left(Re, \frac{\epsilon}{D}, \frac{L}{D}, \lambda \right), \quad (2)$$

where D is the opening diameter of a circular opening and C_d is termed the discharge coefficient. The Reynolds number Re is usually based on the mean velocity and the opening diameter,

$$Re = \frac{QD}{A\nu}. \quad (3)$$

For certain opening geometries, further theoretical progress has been made in expressing C_d in terms of the flow quantities, however, these analyses still draw on an empirical constant $\phi = A_{vc}/A$, the degree of contraction. Measurements show that, for sharp-edged openings ($L/D \ll 1$), $C_d \approx 0.6$ over the wide range of area ratios $\lambda \leq 0.7$ (Ward-Smith [11], pg.392).

These principles of homogeneous fluid flow through orifice plates in pipes are commonly applied even in heterogeneous

fluids. In many cases of practical interest, fluid of one density may flow through an opening into a region of fluid of a different density. A common example is when warm air flows out through an upper opening of a heated room into cooler air outside. While some measurements support the use of $C_d \approx 0.6$ for buoyancy-driven flows through openings in buildings [3], others indicate that the use of a constant value could lead to significant errors in flow rate predictions [4]. However, in these situations, the analogy of a constriction in a pipe may not always be suitable because air flows may be deflected around the building opening, which typically has a geometry far more complex than the circular orifice plates commonly encountered in pipes.

We now consider the effect of a density contrast across an opening. For a horizontal opening, a discharge of buoyant fluid will develop into a plume-like flow if unconfined. Studies on turbulent plumes [8, 2, 6] demonstrate that for a range of source conditions a plume may contract as it rises above the source (figure 1b). The plume contraction is a result of the acceleration of the fluid as it leaves the opening and is entirely due to the action of the buoyancy forces. The degree of plume contraction depends on the initial plume conditions, that is conditions at the discharge opening. For a vertical opening, a discharge of buoyant fluid will also develop into a plume-like flow in the absence of boundaries. However, the initial momentum flux is perpendicular to the momentum flux that is generated by the buoyancy force.

With this in mind, we hypothesise that the presence of a density contrast will have a significant effect on the discharge characteristics of an opening, so that (2) is modified to allow $C_d(Re, \varepsilon/D, L/D, \lambda, \Delta\rho/\rho_0)$. From the arguments above, we expect an enhanced contraction that may yield $C_d < 0.6$. In order to test this hypothesis, a series of experiments were conducted and the dependence of C_d on the source conditions of the discharge deduced. Experiments were conducted in water tanks using salt solutions to create density contrasts. Both horizontal and vertical openings are considered. We restrict our attention to examining the effect of a density contrast on specific opening types, and do not investigate systematic variations with Re , ε/D , L/D or λ . We appeal to plume theory for further insight.

Theoretical plume contraction

A Boussinesq turbulent plume which results from a discharge of buoyant fluid, density $\rho_d = \rho_0 - \Delta\rho$, into quiescent surroundings of constant density ρ_0 may be characterised in terms of the fluxes of volume Q_d , buoyancy B_d and momentum M_d at the discharge opening. The relative importance of these fluxes can be expressed as a dimensionless parameter

$$\Gamma_d = \frac{5}{2^{7/2} \alpha \pi^{1/2}} \frac{Q_d^2 B_d}{M_d^{5/2}}, \quad (4)$$

where α (≈ 0.083) is the plume entrainment coefficient [8,6]. The discharge parameter Γ_d represents the balance between buoyancy and inertial effects at the discharge opening. In the absence of buoyancy, $\Gamma_d = 0$, and as buoyancy effects become increasingly dominant, Γ_d increases. Assuming a uniform velocity profile across the opening, $M_d = Q_d^2/A$ and (4) can be expressed as

$$\Gamma_d = \frac{5}{2^{7/2} \alpha \pi^{1/2}} \frac{A^{5/2} g'_d}{Q_d^2}, \quad (5)$$

where $B_d = Q_d g'_d$, and the reduced gravity is $g'_d = g \Delta\rho/\rho_0$. The solution of the plume conservation equations (Morton, Taylor & Turner [10]) for a release from a horizontal opening subject to the classical entrainment assumption, based on Gaussian profiles across the plume, yields the integral equation for the volume flux as a function of height,

$$\frac{z}{b_0} = \frac{3}{5} \Gamma_d^{-1/5} \int_1^{Q/Q_d} \left(\left(\frac{Q}{Q_d} \right)^2 - \frac{\Gamma_d - 1}{\Gamma_d} \right)^{-1/5} d \left(\frac{Q}{Q_d} \right), \quad (6)$$

see Hunt & Kaye [6], where $b_0 = 5Q_d/3\alpha\pi^{1/2}2^{3/2}M_d^{1/2}$. The plume radius $b(z)$, at height z above the source, can then be expressed as $b(z)/b_0 = \Gamma_d^{-1/5} ((Q(z)/Q_d)^2 - (\Gamma_d - 1)/\Gamma_d)^{-1/5}$. Figure 2 shows the plume radius as a function of z for a range of Γ_d . Caulfield [2] predicts that plumes contract above the source only if $\Gamma_d > 2.5$, as confirmed in figure 3 which shows the minimum plume radius b_{min} as a function of Γ_d . These results suggest that, for horizontally orientated openings, a critical value of Γ_d must be exceeded before the effects of buoyancy begin to alter the discharge characteristics of the openings. As Γ_d increases beyond 2.5, the contraction is more pronounced (also, see Morton & Middleton [9]). Note, from (5), that Γ_d can be increased by increasing the source area and density contrast or by reducing the volume flow rate.

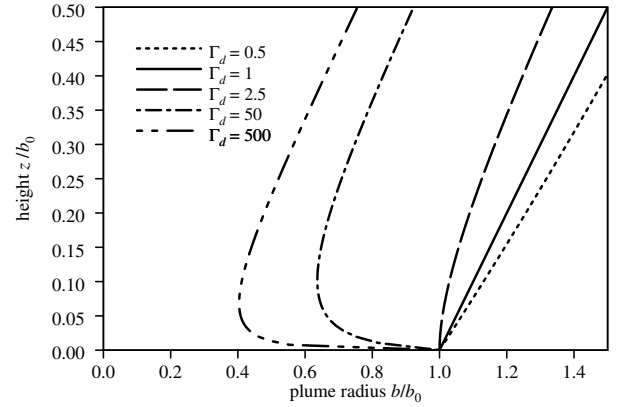


Figure 2. The plume radius $b(z)/b_0$ as a function of distance from the source z/b_0 , for discharge parameters $\Gamma_d = 0.5, 1, 2.5, 50$ and 500 .

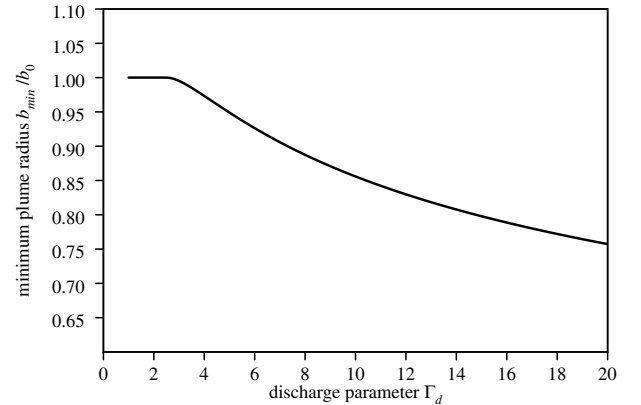


Figure 3. The minimum plume radius b_{min}/b_0 as a function of the discharge parameter Γ_d .

The discharge parameter Γ_d is the only independent non-dimensional group which can be formed from the fluxes Q_d , B_d and M_d . Hence we expect that discharges through openings in vertical surfaces will also be characterised by Γ_d , although the dynamics of the subsequent flow will clearly be very different from the vertically moving plume-like flow described above.

Experiments

A rectangular acrylic container of constant rectangular cross-section S was immersed in a larger water-filled tank. A layer of dense salt solution was introduced in the base of the container, and drained out through one or more openings in the base, while fresh water was drawn in through the top of the container. In the context of the natural ventilation of buildings, this type of flow

is termed a displacement flow. When studying discharges through horizontal openings, circular openings were cut in the base and top of the container and the container top could be completely removed. A smaller number of experiments were used to study discharges through vertical openings, when rectangular slots were opened at the base of a side wall, and the top was left open. The areas of the upper and lower vents will be denoted by a_{upper} and a_{lower} , respectively. In general, $a_{lower} \ll a_{upper}$, and the flow rate through the container was controlled by the discharge through the lower opening [7]. In a few experiments, $a_{lower} = a_{upper}$, and with knowledge of C_d for the lower opening, C_d for the upper opening could be deduced.

Discharges through circular horizontal openings with $D = 5.5\text{cm}$ were carried out in containers with $L = 1\text{cm}$, and $S = 600\text{cm}^2$ or 1600cm^2 . Discharges through vertical openings were carried out in a container with $L = 3.5\text{cm}$, and $S = 1760\text{cm}^2$. The vertical openings were rectangular, with height $l = 4\text{cm}$ and width w in the range $1.25\text{cm} < w < 40\text{cm}$.

Two types of experiment were performed. In the first, the container was initially filled to a depth h_0 with dense saline fluid of a known reduced gravity g'_d , which was allowed to drain. The rate of descent of the interface height h was recorded while the interface remained more than one opening diameter above the opening. For lower interface positions, a mixture of fluid from both above and below the interface is drawn out of the container. The discharge fluxes, and hence Γ_d , vary as the container drains.

In the second type of experiment, a steady two-layer stratification was established by introducing a localised negative buoyancy source in the container, positioned at height H above the base. The experimental set-up is depicted in Hunt & Holford [5]. Saline solution of reduced gravity g'_p was supplied at a constant flow rate Q_p . After an initial transient period, the resulting descending plume supplied a dense layer of steady depth h and uniform steady reduced gravity g'_d . By varying the height H , a range of different steady density stratifications and discharge parameters Γ_d were produced. Measurements were again limited to those experiments in which the interface was more than one opening diameter above the base.

In both types of experiment, the depth h was measured to within 1 mm from digitised images. The density of the ambient, the lower layer and, where used, the plume supply fluid, were measured with an Anton Paar density meter, giving the reduced gravities to an accuracy of $5 \times 10^{-3} \text{cms}^{-2}$. The maximum possible range of reduced gravity was used for the saline layer, with $1 \text{cms}^{-2} < g'_d < 190 \text{cms}^{-2}$. The volume flow rate Q_p of the plume supply was measured with a calibrated inline flowmeter to an accuracy of $8 \times 10^{-2} \text{cm}^3 \text{s}^{-1}$.

In the first type of experiment, Q_d is calculated from the rate of change of interface height, $Q_d = S dh/dt$. In the second type of experiment, Q_d is calculated from conservation of buoyancy, based on the input buoyancy flux at the plume source, $Q_d = Q_p g'_p / g'_d$. The advantage of this method of calculating Q_d is that no account of plume dynamics or origin corrections is necessary. Estimated errors in Q_d by either method are $< 10\%$. The Reynolds number and discharge parameter are calculated from (3) and (5), respectively.

The pressure driving flow through the openings is the excess hydrostatic pressure $\Delta p = \rho_0 g'_d h$ resulting from the dense layer of thickness h . In the situation when there are openings at the top and bottom ($a_{upper} \ll S$), the pressure drop is split between the openings, and (2) must be extended to

$$\frac{Q_d}{\sqrt{2g'_d h}} = \left(\frac{1}{C_{dlower}^2 a_{lower}^2} + \frac{1}{C_{dupper}^2 a_{upper}^2} \right)^{-1/2}, \quad (7)$$

see Linden *et al.* [7]. For $a_{lower} \ll a_{upper}$, the simplification

$$C_{dlower} = \frac{Q_d}{a_{lower} \sqrt{2g'_d h}}, \quad (8)$$

was used, while for $a_{lower} = a_{upper}$, C_{dupper} was deduced from (7).

From (5) and (8), it can be shown that $\Gamma_d \propto a_{lower}^{1/2} h \propto D/h$, for a single circular opening. Hence it is possible that any changes in C_d with Γ_d may be due to a change in the geometric ratio D/h rather than to a change in the balance of fluxes at the outlet opening. To rule out this possibility, a number of experiments were carried out with two equal area openings in the base.

The scaling factors in the definition of Γ_d in (5) are appropriate for an axisymmetric (circular) opening. An equivalent Γ_L can be defined for the fluxes per unit length from a 2D line source. When calculating Γ_d for discharges through rectangular openings, the smaller of the axisymmetric and 2D parameters was chosen, as a means of interpolating smoothly between the two limits. The Reynolds number was based on the mean velocity and the smaller of the width and height of the opening.

Accounting for the use of one or two lower openings in the container, the contraction ratio in these experiments spanned the range $0.006 < \lambda < 0.09$. The horizontal openings were relatively sharp ($L/D = 0.18$) while the vertical openings had significant thickness ($L/l = 0.88$).

Results

Horizontal Openings

The discharge coefficient C_d deduced from the laboratory measurements is plotted as a function of Γ_d in figure 4. Data are taken from draining experiments (+) and from steady-state experiments (\square and \diamond), using either one or two lower openings, respectively. The dependence of C_d on Γ_d is clear and dramatic. For small Γ_d , C_d takes a constant value, within the experimental scatter, whereas for larger Γ_d , C_d decreases as Γ_d increases. An increase in Γ_d from 0 to 15 results in a decrease in C_d of around 33 %.

A least squares best fit to the draining data, in two regions, is

$$C_d = \begin{cases} 0.63 & \text{for } 0 \leq \Gamma_d < 4.9, \\ 1.11 \times \Gamma_d^{-0.356} & \text{for } 4.9 < \Gamma_d < 500. \end{cases} \quad (9)$$

Although the data for $\Gamma_d = 0$ are not shown on this log-log plot, $C_d = 0.63$ in this limit also. This value is consistent with existing measurements, in the absence of a density contrast, for openings with $L/D = 0.18$.

Points representing experiments with one or two base openings follow the same trend, showing that Γ_d , rather than D/h , is the

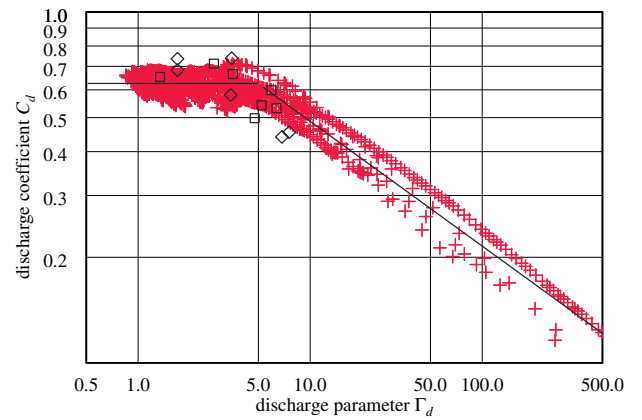


Figure 4. Discharge coefficient C_d as a function of the discharge parameter Γ_d , for experiments with horizontal openings. Draining data for one base opening (+) and steady data for one (\square) and two (\diamond) base openings are shown, together with the best fit line (9).

important parameter. For the draining experiments shown, the Reynolds number lay in the range $200 \leq Re \leq 10000$, while the steady state experiments covered the narrower range $1300 \leq Re \leq 2900$. For each draining experiment, Re falls as Γ_d rises. However, figure 5 shows that there is no collapse in C_d as a function of Re , since the reduction in C_d below the value for a homogeneous, high Re flow is not correlated with Re .

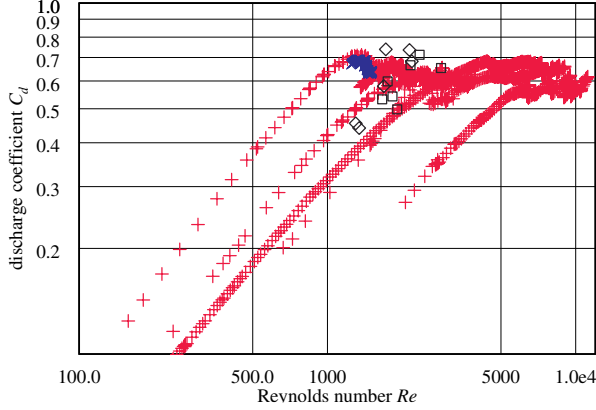


Figure 5. Discharge coefficient C_d as a function of the Reynolds number Re , for experiments with horizontal openings. Draining data for one (+) and two (x) base openings, and steady data for one (□) and two (◇) base openings are shown.

Vertical Openings

The discharge coefficient C_d deduced from the laboratory measurements of draining experiments is plotted as a function of Γ_d in figure 6. The data, for three opening areas comprising two vents, and one comprising a single vent, has collapsed, within experimental error, onto a single curve. In contrast to discharges through horizontal openings, there is a sharp decrease in C_d as Γ_d increases above zero. An increase in Γ_d from 0 to 15 results in a decrease in C_d of around 33 % below the expected value of 0.63. A least squares quadratic fit through these data give

$$C_d = 0.56 \times \Gamma_d^{-0.101}. \quad (10)$$

Reynolds numbers lie in the range $1000 \leq Re \leq 12000$, and again there is no systematic variation with Re .

Conclusions

The discharge coefficient C_d associated with sharply contracting flow through openings in horizontal and vertical surfaces has been measured for a range of density differences across the opening. The measurements show that C_d is dependent on the density contrast $\Delta\rho$ across the opening, through the dimensionless discharge parameter Γ_d , and that large density contrasts may reduce C_d significantly.

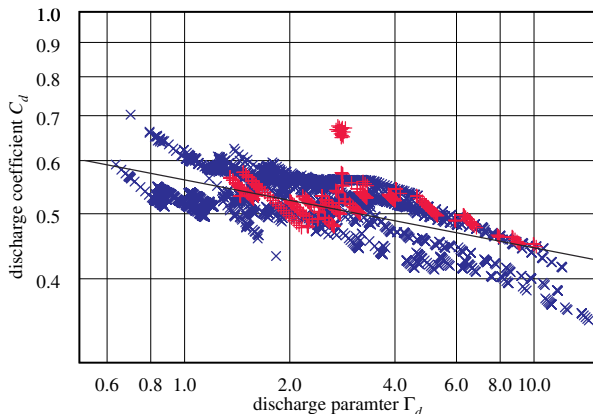


Figure 6. Discharge coefficient C_d as a function of the discharge parameter Γ_d , for draining experiments through one (+) and two (x) vertical base openings, together with the best fit line (10).

A buoyant discharge from a horizontal opening produces a plume-like flow, which may contract considerably in cross section as it rises. This buoyancy-induced contraction is in addition to the inertial contraction and reduces the fraction of the opening area occupied by the discharge, giving rise to reduced values of C_d . The discharge parameter Γ_d provides a measure of the relative importance of buoyancy forces and inertia at the opening. Essentially, discharges with a large value of Γ_d accelerate through the opening because of the local buoyancy contrast, while discharges with a small value of Γ_d are forced out by the imposed pressure difference across the opening. The same discharge parameter may be used to quantify the balance between buoyancy forces and inertia in the flow through a vertical opening.

For small values of Γ_d , buoyancy effects are weak and $C_d \approx 0.6$ is measured. For horizontal openings, once a critical value of $\Gamma_d \approx 5$ is exceeded, buoyancy effects become increasingly important and C_d decreases rapidly with increasing Γ_d . For vertical openings, buoyancy effects are important at all $\Gamma_d > 0$ investigated here, and C_d again decreases with increasing Γ_d .

The dependence of C_d on density contrast implies a potential for significant over-prediction of volume flow rates through constrictions, if a constant value of C_d is assumed when $\Gamma_d \gg 1$. For example, in a ventilated space with horizontal upper and lower openings each of 0.1m^2 connecting to the ambient, a 0.3m deep layer of air 5K warmer than ambient drives a flow rate of $0.013\text{m}^3\text{s}^{-1}$, which discharges with $\Gamma_d = 10$. The flow rate calculated using $C_d = 0.63$ is 16% greater than this true value.

Acknowledgements

JMH & GRH acknowledge the financial support of the Leverhulme Trust and the EPSRC. We would like to thank B. Dean, D. Lipman, C. Mortimer, D. Page-Croft and L. Pratt for their craftsmanship and technical support in the laboratory.

References

- [1] Batchelor, G.K., *An introduction to fluid dynamics*, Cambridge University Press, 1967, 615pp.
- [2] Caulfield, C.P. *Stratification and buoyancy in geophysical flows*. PhD thesis, University of Cambridge, UK, 1991.
- [3] Flourentzou, F., Mass, J. Van Der & Roulet, C.A., Experiments in natural ventilation for passive cooling, in *Proc. 17th AIVC Conf.*, Sweden, 1996, 121–134.
- [4] Heiselberg, P., Svidt, K. & Nielsen, P.V., Windows - measurements of air flow capacity, in *Proc. Roomvent 2000*, UK, editor H.B. Awbi, 2, 2000, 749–754.
- [5] Hunt, G.R. & Holford, J.M. The discharge coefficient - experimental measurement and dependence on density contrast. *Proc. 21st AIVC Conference*, The Hague, Netherlands, 2000.
- [6] Hunt, G.R. & Kaye, N.G., Virtual origin correction for lazy turbulent plumes, *J. Fluid Mech.*, **435**, 2001, 377–396.
- [7] Linden, P.F., Lane-Serff, G.F. & Smeed, D.A., Emptying filling boxes: the fluid mechanics of natural ventilation, *J. Fluid Mech.*, **212**, 1990, 300–335.
- [8] Morton, B. R. Forced plumes, *J. Fluid Mech.*, **5**, 1959, 151–163.
- [9] Morton, B. R. & Middleton, J., Scale diagrams for forced plumes, *J. Fluid Mech.*, **58**, 1973, 165–176.
- [10] Morton, B. R., Taylor, G. I. & Turner, J. S., Turbulent gravitational convection from maintained and instantaneous sources, *Proc. Roy. Soc.*, **234**, 1956, 1–23.
- [11] Ward-Smith, A.J., *Internal fluid flow - the fluid dynamics of flow in pipes and ducts*, Clarendon Press, 1980, 566pp.